Polym. Bull. (2011) 67:1029–1044
DOI 10.1007/s00289-011-0479-y

ORIGINAL PAPER

Thermal and electrical properties of carbon nanotubes based polysulfone nanocomposites

Lalatendu Nayak · M. Rahaman · D. Khastgir · T. K. Chaki

Received: 12 October 2010 / Revised: 21 February 2011 / Accepted: 29 March 2011 /

Abstract Carbon nanotubes (CNTs)-reinforced polysulfone (PSU) nanocomposites were prepared through solution mixing of PSU and different weight percent of multi-walled carbon nanotubes (MWCNTs). Thermal properties of nanocomposites were characterized using thermo-gravimetric analysis (TGA) and differential scanning calorimetry (DSC). TGA studies revealed an increase in thermal stability of the PSU/MWCNTs nanocomposites, which is due to the hindrance of the nanodispered carbon nanotubes to the thermal transfer in nanocomposites and also due to higher thermal stability of CNTs. Morphological properties of nanocomposites were characterized by high resolution transmission electron microscopy (HRTEM) and field emission scanning electron microscope (FESEM). The influence of CNTs loading on electrical properties of PSU/MWCNTs nanocomposites was studied by the measurement of AC and DC resistivity. Dielectric study of nanocomposites was carried out at different frequencies (10 Hz–1 MHz) by using LCR meter. An increase in dielectric constant and dielectric loss was observed with increase in CNTs content, which is due to the interfacial polarization between conducting CNTs and PSU.

Keywords Carbon nanotubes · Thermal properties · Morphology · Electrical conductivity

Introduction

Polymer nanocomposites have emerged as a distinct field in modern nanotechnology due to their remarkable properties like lightweight, extremely improved mechanical, thermal, physical, electrical, and magnetic properties. These ideal

---

L. Nayak · M. Rahaman · D. Khastgir · T. K. Chaki (✉)
Rubber Technology Centre, Indian Institute of Technology, Kharagpur 721302, India
e-mail: tapanchaki2009@gmail.com; tapan@rtc.iitkgp.ernet.in

enhanced properties are due to ultrahigh interfacial area of the nanosized particles that can permit strong interaction with the polymer matrix. Among all nanofillers, carbon nanotube (CNT) is the best reinforcing nanofiller for high performance and multifunction polymer nanocomposites in the twenty-first century due to their high stiffness and mechanical strength (stronger than steel), high electrical and thermal conductivity (more conductive than copper), light weight, low density, low melt flow viscosity (lighter than aluminum).

A number of works on polymer/CNTs nanocomposites have been carried out taking different polymer matrices in order to enhance their different properties. CNTs based polymer composites, including matrices such as polyethylene (PE) [1], polypropylene (PP) [2], poly(methyl methacrylate) (PMMA) [3] and polyamide [4] and polyurethane [5, 6], have been studied. Liu et al. [7] prepared multi-walled carbon nanotubes (MWCNTs)/polyimide (PI) composites by in situ polymerization and stated that, with the incorporation of 1 wt% MWCNTs, the elastic moduli of nanocomposites was significantly improved about 248% while the tensile strength was comparable to that of neat PI matrix. Park et al. [8] stated that with the addition of 3 wt% of MWCNTs in PMMA, the electrical resistivity was decreased from 10^{15} to 10^{2} Ω-cm. Chou et al. [9] prepared polyimide nanocomposites taking plasma modified MWCNTs and stated that by the addition of 0.5 wt% of MWCNTs, tensile strength was increased up to 120% and modulus up to 110%.

Incorporation of conductive filler in insulating polymer matrix can produce a conductive composite when concentration of conducting phase exceeds certain critical concentration known as percolation threshold. According to percolation theory, a filler with higher aspect ratio will have a lower percolation threshold and a better transfer of properties to the polymer [10]. The high aspect ratio, low density, high tensile strength (order of 200 GPa—100 times of steel), high resilience, high current carrying capacity, very low percolation threshold ($\sim$0.05–2 wt%), high heat transmission, and high thermal stability of CNTs make them excellent filler for preparation of conducting composites [9]. A “percolation threshold” of 0.5 v% for MWCNTs was reported in the literature [11]. However, this value again depends on type of CNTs used, for example, for SWCNTs percolation is around 0.1 wt% [12].

Due to high aspect ratio of the CNTs, the chance of contact increases, which reduces the percolation threshold so that conduction occurs at much lower loading compared to other conducting fillers like carbon black and carbon fiber without affecting the other properties of the polymer [12].

Electrical conductivity of a composite is significantly affected by interaction between CNTs and polymer matrix, the properties of CNTs themselves (purity, diameter, length, specific surface area, surface conductivity), and the dispersion of CNTs within the polymer. It is also dependent on the matrix material or the preparation process used. Barrau et al. [13] have developed a composite on epoxy resin which exhibited a percolation threshold at 0.3 wt% of SWCNTs. Transport properties in SWCNTs and MWCNTs–PMMA composites have been reported by Benoit et al. [14] and Stephan et al. [15], where low percolation thresholds of 0.33 and 0.5 wt% were obtained. Very recently, Isayev et al. [16] reported a new method to effectively disperse the self functionalized MWCNTs in the polyetherimide (PEI). They observed a sharp reduction in resistivity at 2 wt% MWCNTs content indicating that the percolation threshold lies between 1.0 and 2.0 wt% MWCNTs loading.

The conductivity of a polymer composite depends upon inter-particle distance of conducting fillers in polymer matrix. Three main factors like dispersion, aspect ratio, and alignment of conducting filler influence the percolation threshold for electrical conductivity in polymer composites [17]. Although polymer/CNTs nanocomposites hold great promise, their dispersion and the weak interface between the nanotubes and the polymer matrices are critical issues for successful applications. To improve the CNTs dispersion in polymer matrix, several approaches have been proposed including the direct suspension of CNTs in the polymer solution via ultrasonication [18, 19], the in situ polymerization in the presence of CNTs [20, 21], and the chemical modification of CNTs for their solubilization [22, 23]. Good dispersion of CNTs in polymer matrix depends on the force of attraction between CNTs and polymer matrix, but high force of attraction between CNTs and polymer matrix depends upon functionality of CNTs. Numerous research works have been done on functionalization of CNTs. The disadvantages of this approach include that the treatment methods were generally poorly controlled and time/energy consuming, which give inconsistent results in the performance of nanocomposites. In addition, the treatments of CNTs including purification, oxidation, and various functionalization magnified the cost of CNTs and also the chemical treatment of CNTs reduces the electrical conductivity of nanocomposites due to change in Fermi level and debonding of nanotubes [24]. All of these limited the adoption of new materials and their standard fabrication processes in industry. In our study, we have designed a very simple solution mixing process using ultrasonication to improve dispersion of received MWCNTs in polysulfone (PSU) to achieve low percolation threshold.

Polysulfone (PSU), a transparent engineering plastic with good film formation property is used typically in medical, food processing equipment, electrical and electronics components [25]. Very few works have been reported on PSU/CNTs nanocomposites for membrane preparation, but no work is reported on effect of CNTs loading on electrical, thermal, and morphological properties of PSU. Main purpose of the present work is to develop thin film composites with good electrical conductivity for the mitigation of electrostatic charge accumulated on the surface of the films used in packaging and also to develop high dielectric material for charge storage devices. In this study, PSU/CNTs thin film nanocomposites were prepared through a new simple solution mixing process to investigate the effect of CNTs loading on different properties of PSU/MWCNTs nanocomposites.

Experimental

Materials

Polysulfone (PSU) in powder form (Grade Udel P-1700) was supplied by Solvay Advanced Polymers. MWCNTs used in this study were purchased from Helix Material Solution, USA and used as received. MWCNTs were prepared by the chemical vapor deposition process having carbon content of about 95%, average diameter of about 40–60 nm and length of about 0.5–40 μm. Chloroform has been used as a solvent for PSU and was purchased from Merck Specialties Private Limited, India.

Preparation of nanocomposite films

Prior to film preparation PSU was dried in an oven at 135 °C for 6 h and MWCNTs were dried at 120 °C for 24 h. Nanocomposite films were prepared through solution mixing process. First, given amount of CNTs was dissolved in chloroform by sonication for 1 h in a sonicator. Then required amount of PSU dissolved in chloroform was added to CNTs dispersed solvent and the mixed solution was stirred and sonicated for 1 h and 30 min. Stirring and sonication were done in 5 min interval. Thin films of average thickness 50–60 μm were prepared by casting the solution and evaporating the solvent at room temperature for overnight, followed by 60 °C for 2 h, 120 °C for 1 h, 150 °C for 1 h to remove solvent completely. Figure 1 describes the procedure for making polymer nanocomposite films.

Characterizations

Thermo-gravimetric analysis (TGA) was performed using a TA Instruments TGA Q50 V6.1, USA under a nitrogen atmosphere from room temperature to 700 °C operated at a heating rate of 20 °C/min using samples weight about 8–10 mg.

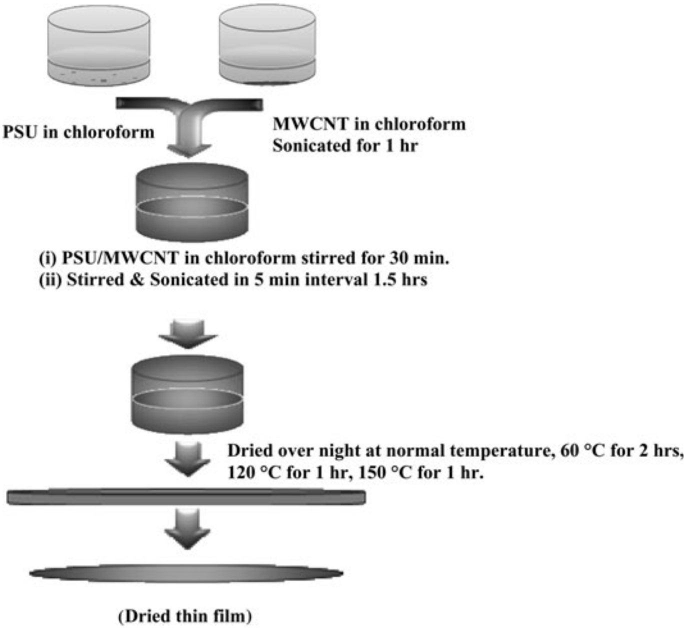

Fig. 1 Process used for making PSU/MWCNTs nanocomposites thin film

Differential scanning calorimetry (DSC) was carried out in a TA instruments machine DSC Q100 in N_2 atmosphere from 50–350 °C heated at a rate of 10 °C/min. The distribution of CNTs into the PSU matrix and interfacial region of CNTs and matrix were studied using a high resolution transmission electron microscope (HRTEM, JEM 2100, JEOL Limited, Tokyo, Japan) attached with charge couple device (CCD) camera (Gatan, Inc., CA, USA). The specifications for HRTEM were point to point resolution of 0.194 nm, lattice resolution of 0.14 nm, 24° tilt angle, accelerated voltage of 200 keV and electron gun of lanthanum hexaboride (LaB6) filament type. The samples for HRTEM analysis were prepared using an ultramicrotomy with a Leica Ultracut UCT (Leica Microsystems GmbH, Vienna, Austria). Freshly sharpened diamond knives with cutting edges of 45° were used to obtain cryosections of 50–60 nm thickness specimens at ambient temperature. The cut samples were supported on a copper mesh before observation under the microscope. The nanostructure morphology of the PSU/MWCNTs nanocomposites was evaluated using field emission scanning electron microscope (model Supra 40, Carl Zeiss SMT AG, Oberkochen, Germany). Samples were gold coated by means of manually operated sputter coater (model SC7620, Polaron Brand, Quorum Technologies Ltd., East Sussex, UK) unit. The DC resistivity of the nanocomposites having the resistivity greater than 10^6 Ω-cm were measured using Hewlett Packard (Model 16008A) resistivity cell coupled with a Hewlett Packard HP 4329A resistance meter. DC resistivity of the nanocomposites having the resistivity less than 10^6 Ω-cm was measured using DC milli-ohm meter (model no.GOM-802, Goodwill Instek Co., Taiwan). AC resistance was directly measured using a LCR meter (Model 819, Goodwill Instek Co., Taiwan) over the frequency range 10 Hz to 1 MHz. Study of the dielectric properties were carried out using LCR meter over the frequency range 10 Hz to 1 MHz. Dielectric constants and dielectric loss of the nanocomposites were measured using the following equations:

$$\text{Dielectric constant}(\varepsilon') = Ct/0.0885\ \text{A} \tag{1}$$

where C is the capacitance in picofarad, t is the thickness of sample in cm, A is the area of the sample in cm^2

$$\text{Dielectric Loss}(\varepsilon'') = \text{Dielectric Constant} \times \text{Dissipation Factor} \tag{2}$$

Results and discussion

Thermal properties of the PSU/MWCNTs nanocomposites

TGA Studies

The TGA results of PSU and its nanocomposites in an environment of nitrogen are presented in Table 1 and Fig. 2a and b. In case of pure PSU, onset thermal degradation temperature is 531 °C, but after MWCNT loading, thermal stability was increased up to 3 wt% MWCNTs loading, where onset degradation temperature is 537 °C. This enhancement in thermal stability may be due to the hindrance of the

Table 1 Thermal data from thermo gravimetric analysis

Composition	T_5 (°C)	T_{10} (°C)	T_{20} (°C)	T_{30} (°C)	T_{50} (°C)	T_{max} (°C)
S0 (PSU + 0% CNTs)	531	544	556	563	574	563
S1 (PSU + 1% CNTs)	535	548	559	566	580	568
S3 (PSU + 3% CNTs)	537	551	562	569	587	569
S5 (PSU + 5% CNTs)	531	545	556	563	582	563.5

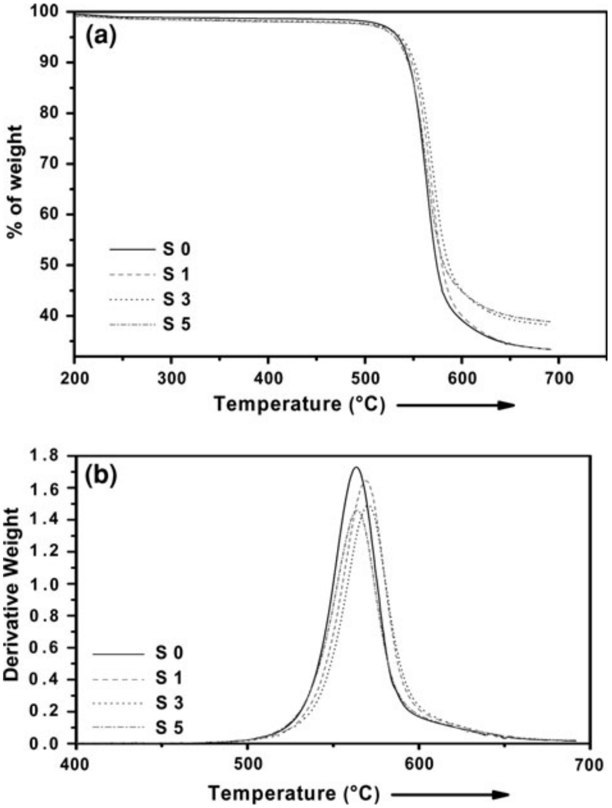

Fig. 2 **a** TGA curves of PSU/MWCNTs nanocomposites. **b** DTG curves of PSU/MWCNTs nanocomposites

nanodispersed CNTs to the thermal transfer in the matrix and also due to hydrogen bonding between CNTs and PSU. Simultaneously, confinement of PSU polymer chains onto the surface of CNTs restricted the segmental motion of polymer and suppressed the chain transfer reaction. From TGA thermogram, it is also seen that temperature at 10%, 20%, 30%, and 50% weight loss for PSU/MWCNTs nanocomposites is somewhat higher than as compared to pure PSU. When CNTs loading is more than 3 wt%, thermal stability is decreased to a small extent due to the entrapment of used solvent between CNTs and PSU and less force of attraction between CNTs and PSU. This entrapment of solvent is mainly due to strong van der Waals force of attraction between solvent and CNTs [26]. Figure 2b shows the DTG curves of PSU and its nanocomposites. From Fig. 2b it is seen that the temperature at maximum degradation rate, i.e., peak temperature of PSU/MWCNTs nanocomposites shifts towards higher temperature with increase in MWCNTs content. Peak temperature of pure PSU is 563 °C, while the values are 568, 569, and 564 °C at loading of 1, 3, and 5 wt% MWCNTs, respectively.

DSC studies

Differential scanning calorimetry (DSC) thermograms of PSU and its nanocomposites are shown in Fig. 3, where pure PSU shows glass transition temperature (T_g) at 186 °C, but after addition of MWCNTs, T_g of nanocomposites is shifted to higher temperature. Glass transition temperature of a polymer composite depends upon the free volume and the affinity between the filler and polymer matrix in the composites. A polymer with a lower free volume with higher affinity to filler shows higher T_g. A polymer matrix with a higher affinity to filler exhibits less molecular motion and reduced free volume of the polymer molecules [27, 28]. In this study, after addition of MWCNTs, T_g is increased up to 190 °C on 3 wt% of MWCNTs. This slight increase in T_g may be due to close affinity between PSU and MWCNTs by inter-molecular hydrogen bonding in the interphase between MWCNTs and PSU.

Morphological structure of the PSU/MWCNTs nanocomposites

HRTEM

Reinforcing effect of nanofillers in a polymer matrix depends on its degree of dispersion in polymer matrix. So the morphological study is very much important for the evaluation of CNTs dispersion in the polymer matrix. To study the dispersion of MWCNTs in PSU matrix, morphology of the PSU/MWCNTs

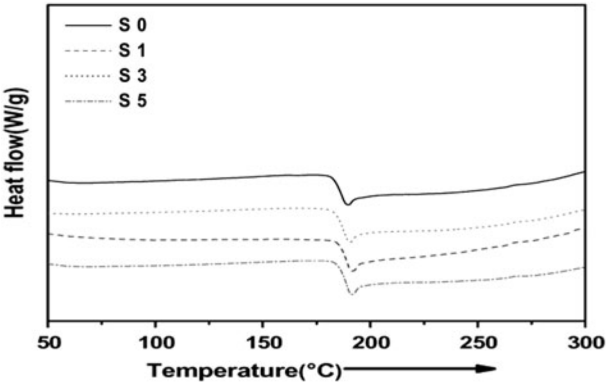

Fig. 3 DSC curve of PSU/MWCNTs nanocomposites

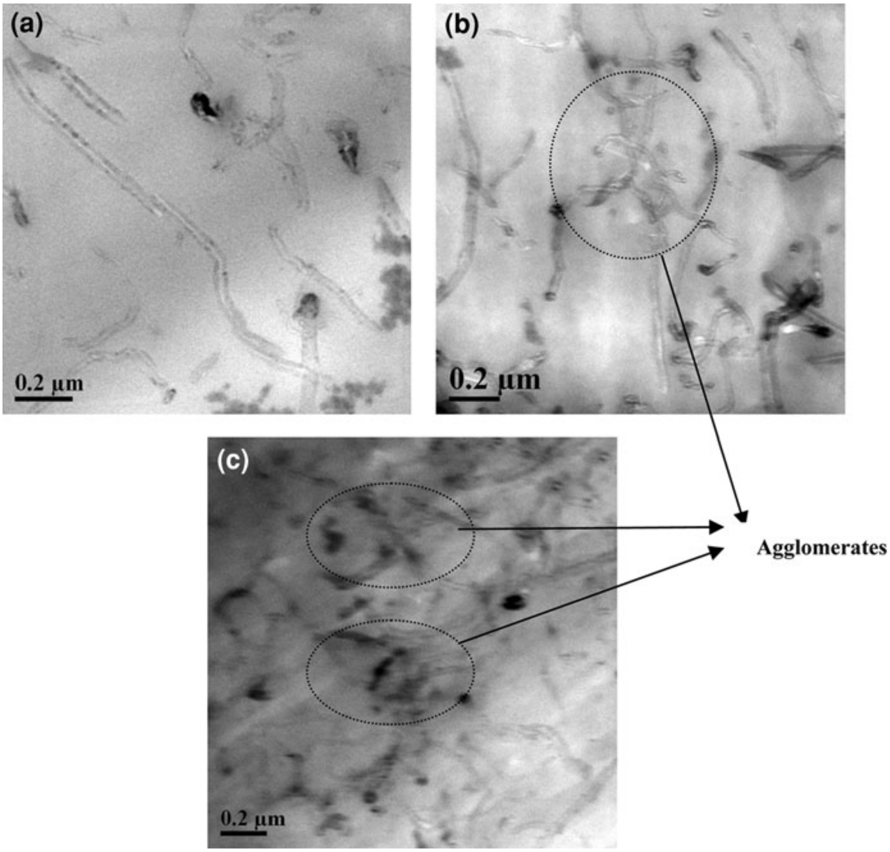

Fig. 4 HRTEM image of **a** S1 (PSU + 1 wt% MWCNTs), **b** S3 (PSU + 3 wt% MWCNTs), **c** S5 (PSU + 5 wt% MWCNTs)

nanocomposites is investigated by HRTEM. HRTEM micrographs of 1, 3, and 5 wt% of MWCNTs in PSU are presented in Fig. 4a, b, and c. Figure 4a shows an abundance of well-dispersed nanotubes throughout the entire PSU matrix without any agglomerates. From micrograph in Fig. 4b, it is seen that dispersion of CNTs is inferior due to presence of some agglomerates of CNTs which are shown in marked circles. These agglomerates reduce reinforcing effects of CNTs because, they act as flaws in polymer matrix. This is why poorly dispersed CNTs in polymer matrix give lower properties than well dispersed one. Figure 4c shows the 5 wt% MWCNTs loading, where high agglomerates of CNTs are seen with the formation of high electrical network.

FESEM

To observe the dispersion and distribution of the CNTs and their physical interaction with the PSU matrix, the FESEM microphotographs of cryo-fractured

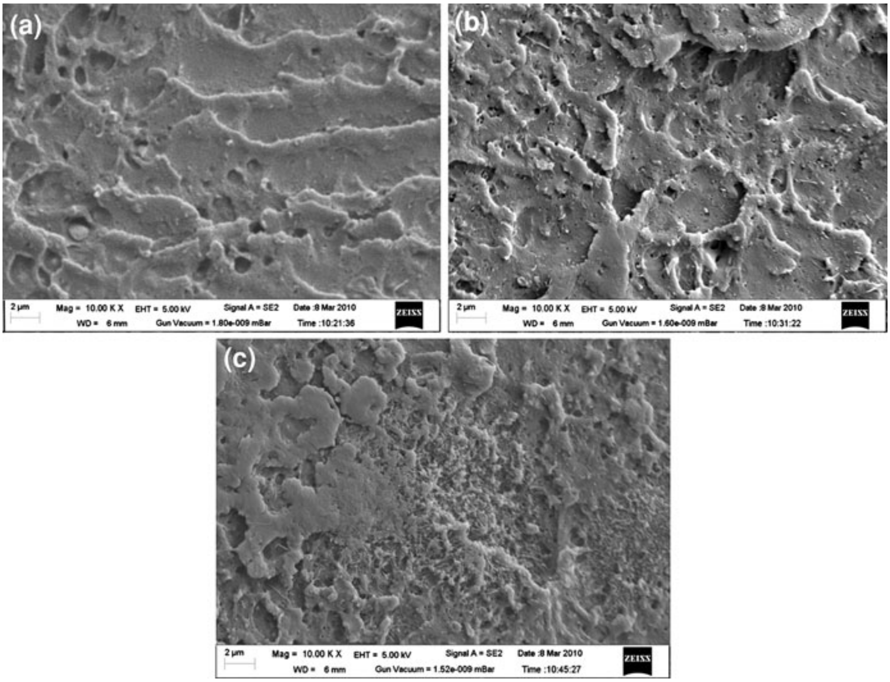

Fig. 5 Cryo-fractured FESEM image of **a** PSU + 1 wt% MWCNTs, **b** PSU + 3 wt% MWCNTs, **c** PSU + 5 wt% MWCNTs

surface morphology of the PSU/MWCNTs nanocomposites are shown in Fig. 5. The bright dots and tread-like structures in the images are attributed to the MWCNTs. It is apparent from Fig. 5 that there are more bright dots and thread-like structures in the composites with higher MWCNTs loading. The dispersion of MWCNTs in the PSU matrix is clearly observed from FESEM images with low magnification that CNTs at lower loading (1 and 3 wt%) are homogeneously dispersed throughout the PSU matrix, but high agglomeration is seen at higher (5 wt%) loading. Micrographs 5a with 1 wt% and (b) with 3 wt% show an abundance of well-dispersed nanotubes throughout the entire surface without any agglomerates. From two micrographs, it seems that induced van der Waals force between the polymer and CNTs during sonication exceeds the existing inter-tube forces. In micrograph 5c, high agglomeration of CNTs is seen, which may be due to self-aggregation of CNTs by van der Waals bonding and also due to lack of interfacial adhesion between CNTs and PSU.

Electrical properties of PSU/MWCNT nanocomposites

DC resistivity

DC volume resistivity of pure PSU and its nanocomposites at different weight percent of MWCNTs loading are presented in Fig. 6. From Fig. 6, it is confirmed

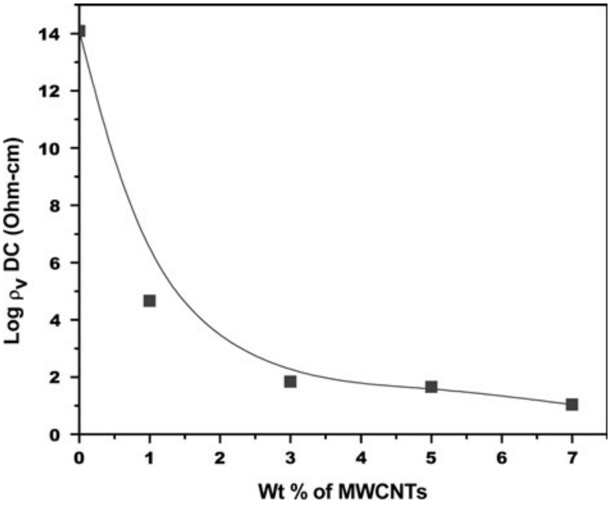

Fig. 6 Effect of CNTs loading on DC volume resistivity of PSU/MWCNTs nanocomposites

that pure PSU is insulative in nature having resistivity greater than 10^{14} Ω-cm, but resistivity is decreased sharply up to 10^{4} Ω-cm with the addition of 1 wt% of CNTs loading. The loading weight percentage at which there is significant decrease in resistivity and beyond which there is marginal decrease is called the percolation limit. In the present work, percolation limit is occurred in-between 1 and 3 wt% of CNTs loading. At lower filler loadings, filler particles act like conductive islands in a sea of electrically insulating polymer [29]. When more filler particles are added, the conductive particles become more crowded and are more likely to come in contact with each other. At percolation threshold, a majority of filler particles are in contact with at least two of their nearest neighbors, thereby forming a continuous conductive chain or network. Prior to percolation limit, conductive particles were dispersed apart from each other in the PSU without forming any conductive path for passage of current, whereas above the percolation, a continuous network of CNTs are formed enabling the current to pass through, thus making the system conductive. The decrease in resistivity at high loading of MWCNTs is due to increase in density of MWCNTs–MWCNTs junctions, which promote the formation of conductive network.

AC resistivity

Effect of frequency on the AC resistivity of pure PSU and its nanocomposites at different weight percent of MWCNTs loading are presented in Fig. 7. From Fig. 7, it is observed that the nanocomposites near the percolation limit show a frequency dependent region and a frequency independent region. Resistivity of the nanocomposites at and above the percolation exhibits frequency independent nature in the measured frequency range. Resistivity of pure PSU and nanocomposites having CNTs loading 1 wt% is appeared to be proportional to frequency due to the

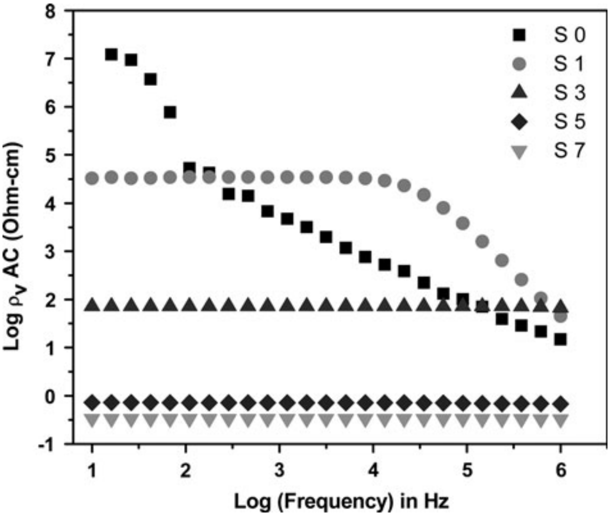

Fig. 7 Effect of frequencies on the AC resistivity of the nanocomposites with different weight percent of CNTs loading

capacitance of the host medium between the conducting particles or aggregates. Also in this nanocomposite, the continuous conductive network has just started to form with many CNTs particles coming close to each other, which give rise to appreciable decrease in resistivity. This can be explained as follows. At high frequencies, the electrons get sufficiently excited so that they can hop from one conducting cluster to another adding to the conductivity already existing because of the smaller interparticle gap. This leads to the decrease in resistivity of these nanocomposites after a critical frequency [30]. When MWCNTs loading was increased to higher weight percent than percolation limit, no significant influence of frequencies on resistivity was observed because of the formation of good electrical network by CNTs.

Dielectric properties

Effect of frequency on dielectric constant The effect of frequency variation on dielectric constant of PSU/MWCNTs nanocomposites at room temperate is presented in Fig. 8. The addition of CNTs to PSU has a dramatic effect on the measured dielectric constant. It is noteworthy that dielectric constant of pure PSU is independent of frequency, but dielectric constant is fully dependent on frequency when CNTs are loaded to PSU as shown in Fig. 8. In this study, when CNTs content is more than 1 wt%, a pronounced dependence of dielectric constant on frequency is observed. In the CNTs loaded system, dielectric constant is sharply decreased with the increase of frequency. Similar results have been reported by many researchers. Dang et al. [31] have reported a reduction in dielectric constant (ε') with increase in frequency for polyvinylidene fluoride and multiwall CNTs. Renukappa et al. [32] have noticed a similar behavior in conductive carbon black filled SBR rubber. When

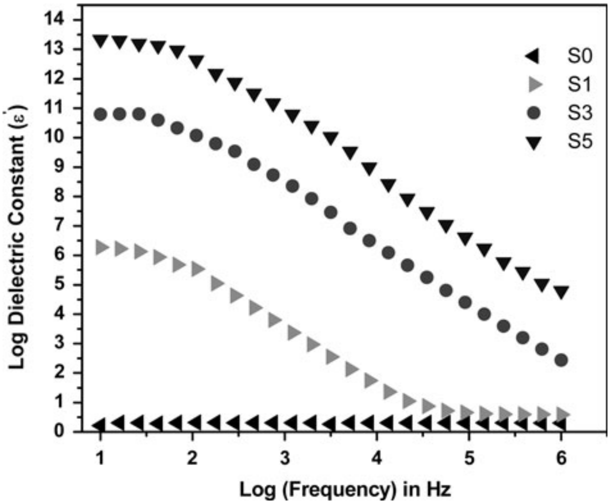

Fig. 8 Effect of frequency on the dielectric constant of the nanocomposites with different weight percent of CNTs loading

MWCNTs loading is 1 wt%, dielectric constant of nanocomposites ε′ is decreased sharply in the range from 10 to 10^6 Hz. This suggests that at the percolation threshold, the established percolation network which consisted of PSU–MWCNTs nearly touching each other, but still remaining electrically insulated because of the existence of a thin insulating polymer layer, is not stable and is easily damaged by external frequency disturbance. Therefore, a remarkable dielectric relaxation is induced with an increase in frequency from 10 to 10^6 Hz. The sharp decrease in dielectric constant with increase in frequency in more MWCNTs loaded nanocomposites may be attributed to a large leakage of current resulted in nanocomposites when an electric field is applied. At low frequency, a high value of ε′ is observed, because at low frequencies, polarization follows the change of electric field (i.e. high polarization of molecules takes place when electric field is applied) and dielectric loss is minimum and the contribution to the dielectric constant is maximum. At high frequencies electric field changes too fast for the polarization effects to appear (i.e., less polarization). So ε′ is minimal at high frequency [33].

Effect of CNTs concentration on dielectric constant The influence of CNTs loading on dielectric properties of PSU/MWCNTs nanocomposites is presented in Fig. 9 at different frequencies. The addition of CNTs to PSU has a dramatic effect on the dielectric properties of PSU nanocomposites. With the increase in CNTs loading, dielectric constant is increased gradually. When weight percent of CNTs increases from 0 to 5 wt%, dielectric constant increases nearer to 9 orders at 3 kHz frequency. This increase in dielectric constant with increase in CNTs loading is mainly due to the interfacial polarization between conducting CNTs and PSU. The difference in conductivity between PSU and CNTs is responsible for occurrence of interfacial polarization. The interfacial polarization leads to an increase in ε′ due to

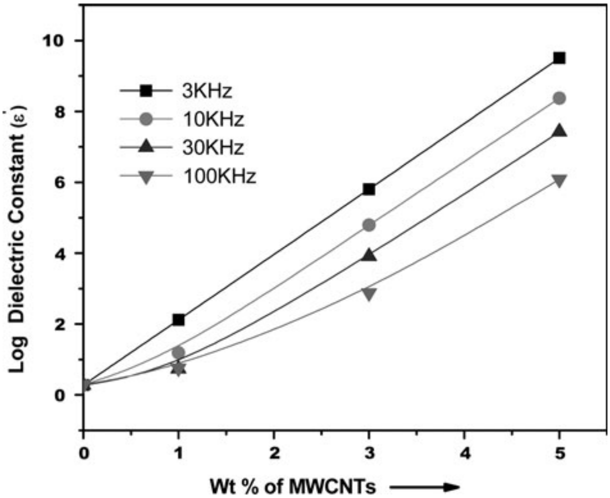

Fig. 9 Effect of carbon nanotubes concentration on the dielectric constant of the PSU/MWCNTs nanocomposites

motion of virtual charges, which get trapped at the interface of the components of a multiphase material of different conductivity [34]. As CNTs content increases, the interfacial polarization and the formation of a conductive network of CNTs increases in the composites and this could be the reason for increase of dielectric constant.

Effect of frequency and CNTs concentration on dielectric loss The changes in dielectric loss of PSU/MWCNTs nanocomposites with respect to frequencies and

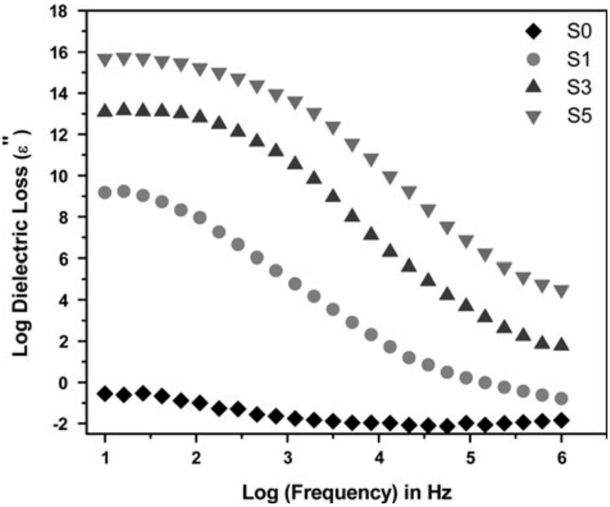

Fig. 10 Effect of frequency on the dielectric loss of the nanocomposites with different weight percent of CNTs loading

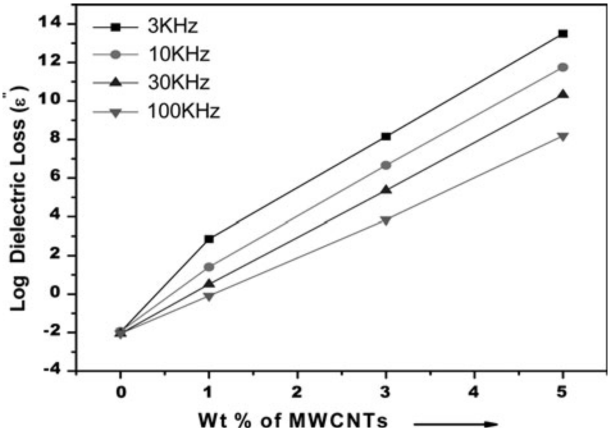

Fig. 11 Effect of carbon nanotubes concentration on the dielectric loss of the PSU/MWCNTs nanocomposites

CNTs concentration are presented in Figs. 10 and 11. The dielectric loss (ε″) is related to relaxation phenomenon and it is the measure of the exponential decay of polarization with time [35]. From Fig. 10 it is confirmed that there is a gradual reduction in dielectric loss with increase in frequency. This is because; the induced charge gradually fails to follow the reversing field causing a reduction in the electric oscillations as the frequency is increased [33]. Figure 11 indicates that with the increase in MWCNTs loading, there is a steep increase in dielectric loss. At low CNTs loading the average distance among conducting particles in insulating matrix are substantially high and composites exhibit marginal frequency independency for dielectric loss.

Conclusions

Thin films of PSU/MWCNTs nanocomposites with unique combination of properties have been developed through solvent casting process. From HRTEM, it is confirmed that solvent casting technique is a noble technique for high dispersion of CNTs. HRTEM study confirmed the uniform dispersion of CNTs throughout the PSU. TGA study reveals that with the addition of MWCNTs thermal stability is increased up to certain extent. DC resistivity of pure PSU is decreased from 10^{14} Ω-cm to 10^{4} Ω-cm after addition of 1 wt% MWCNT and further decreased to 10^{2} Ω-cm with the increase in CNTs content to 7 wt%. PSU/MWCNTs nanocomposites exhibit remarkably enhanced dielectric constant over pristine PSU, so these nanocomposites can be utilized in electrostatic discharge (ESD) application, charge storing devices, decoupling capacitors.

Acknowledgments The financial support of this work provided by Kalpana Chawla Space Technology Cell, IIT–Kharagpur is gratefully acknowledged.

References

1. Tang W, Santare MH, Advani SG (2003) Melt processing and mechanical property characterization of multi-walled carbon nanotubes/high density polyethylene (MWNT/HDPE) composite films. Carbon 41:2779–2785
2. Teng CC, Huang YW, Yuen SM, Weng CC, Chen CH, Su SF (2008) Effect of MWCNT content on rheological and dynamic mechanical properties of multiwalled carbon nanotube/polypropylene composites. Composites A 39:1869–1875
3. Jia Z, Wang Z, Xu C, Liang J, Wei B, Wu D, Zhu S (1999) Study on poly (methyl methacrylate)/carbon nanotube composites. Mater Sci Eng A 271:395–400
4. Cadek M, Le Foulgoc B, Coleman JN, Barron V, Sandler J, Shaffer MSP, Fonseca A, Van ESM, Schulte K, Blau WJ (2002) Structural and electronic properties of molecular nanostructures. AIP Conf Proc Austria 633:562–565
5. Chiang KH, Ping CW, Ming YS, Ho WH, Ming LT (2005) Synthesis, thermal, mechanical and rheological properties of multiwall carbon nanotube/waterborne polyurethane nanocomposites. Compos Sci Technol 65:1703–1710
6. Ma CCM, Huang YL, Kuan HC, Chiu YS (2005) Preparation and electromagnetic interference shielding characteristics of novel carbon nanotube/siloxane/poly-(urea urethane) nanocomposites. J Polym Sci B 43:345–3458
7. Liu TX, Tong YJ, Zhang WD (2007) Preparation and characterization of carbon nanotube/polyetherimide nanocomposites films. Compos Sci Technol 67:406–412
8. Park WK, Kim JH, Lee SS, Kim J, Lee GW, Park M (2005) Effect of carbon nanotube pre-treatment on dispersion and electrical properties of melt mixed multi-walled carbon nanotubes/poly (methyl methacrylate) composites. Macromol Res 13:206–211
9. Chou WJ, Wang CC, Chen CY (2008) Characteristics of polyimide-based nanocomposites containing plasma-modified multi-walled carbon nanotubes. Compos Sci Technol 68:2208–2213
10. Jiang X, Bin Y, Matsuo M (2005) Electrical and mechanical properties of polyimide–carbon nanotubes composites fabricated by in situ polymerization. Polymer 46:7418–7424
11. Kuan CF, Kuan HC, Chen CH (2008) Mechanical and electrical properties of multi-wall carbon nanotube/poly(lactic acid) composites. J Phys Chem Solids 69:1395–1398
12. Ramasubramaniam R, Chen J, Liu H (2003) Homogeneous carbon nanotubes/polymer composites for electrical applications. Appl Phys Lett 83:2929–2930
13. Barrau S, Demont P, Peigney A, Laurent C, Lacabanne C (2003) DC and AC conductivity of carbon nanotubes–polyepoxy composites. Macromolecules 36:5187–5194
14. Benoit JM, Corraze B, Lefrant S, Blau WJ, Bernier P, Chauvet O (2001) Transport properties of PMMA-carbon nanotubes composites. Synth Met 121:1215–1216
15. Stephan C, Phap TN, Lahr B, Blau W, Lefrant S, Chauvet O (2002) Raman spectroscopy and conductivity measurements on polymer-multiwalled carbon nanotubes composites. J Mater Res 17:396–400
16. Isayev AI, Kumar R, Lewis TM (2009) Ultrasound assisted twin screw extrusion of polymer nanocomposites containing carbon nanotubes. Polymer 50:250–260
17. Park C, Ounaies Z, Watson KA, Crooks RE, Smith JJ, Lowther SE, Connell JW, Siochi EJ, Harrison JS, Clair TLS (2002) Dispersion of single wall carbon nanotubes by in situ polymerization under sonication. Chem Phys Lett 364:303–308
18. Curran SA, Ajayan PM, Blau WJ, Carroll DL, Coleman JN, Dalton AB, Davey AP, Drury A, McCarthy B, Maier S, Strevens A (1998) A composite from poly(*m*-phenylenevinylene-*co*-2,5di-octoxy-*p* phenylenevinylene) and carbon nanotubes: a novel materials for molecular optoelectronics. Adv Mater 10:1091–1093
19. Chen J, Liu H, Weimer W, Halls MD, Waldeck DH, Walker GC (2002) Noncovalent engineering of carbon nanotube surfaces by rigid, functional and conjugated polymers. J Am Chem Soc 124:9034–9035
20. Tang BZ, Xu H (1999) Preparation, alignment, and optical properties of soluble poly(phenylacetylene) wrapped carbon nanotubes. Macromolecules 32:2569–2576
21. Barraza HJ, Pompeo F, Rear EA, Resasco DE (2002) SWNT-filled thermoplastic and elastomeric composites by miniemulsion polymerization. Nano Lett 2:797–802
22. Grady BP, Pompeo F, Shambaugh RL, Resasco DE (2002) Nucleation of polypropylene crystallization by single walled carbon nanotubes. J Phys Chem B 106:5852–5858

23. Zhu J, Kim JD, Peng H, Margrave JL, Khabashesku VN, Barrera EV (2003) Improving the dispersion and integration of single walled carbon nanotube in epoxy composites through functionalization. Nano Lett 3:1107–1113
24. Duesberg GS, Muster J, Byrne HJ, Roth S, Burghard M (1999) Towards processing of carbon nanotubes for technical applications. Appl Phys A 69:269–274
25. Stevens MP (1999) In polymer chemistry: an introduction, 3rd edn. Oxford University Press, Oxford, p 311
26. Vaudreuil S, Labzour A, Ray SS, Mabrouk KE, Bousmina M (2007) Dispersion characteristics and properties of poly(methyl methacrylate)/multi-walled carbon nanotubes nanocomposites. Nanosci Nanotechnol 7:2349–2355
27. Chipara MI (1997) The glass transition phenomenon in macromolecular systems. Physica B 234–236:263–265
28. Sperling LH (2001) Introduction to physical polymer science, 3rd edn. Wiley, New York, NY, USA
29. Saleem A, Frormann L, Iqbal A (2007) Mechanical, thermal and electrical resistivity properties of thermoplastic composites filled with carbon fibers and carbon particles. J Polym Res 14:121–127
30. Psarras GC, Manolakaki E, Tsangaris GM (2003) Dielectric dispersion and ac conductivity in-iron particles loaded-polymer composites. Composites A 43:1187–1198
31. Dang ZM, Wang L, Yin Y, Zhang Q, Lei Q (2007) Giant dielectric permittivities in functionalized carbon-nanotube/electroactive-polymer nanocomposites. Adv Mater 19:852–857
32. Renukappa NM, Siddaramaiah, Samuel RDS, Rajan JS, Lee JH (2009) Dielectric properties of carbon black: SBR composites. Mater Sci Mater Electron 20:648–656
33. Panwar V, Kang B, Park J, Park S, Mehra RM (2009) Study of dielectric properties of styrene-acrylonitrile graphite sheets composites in low and high frequency region. Eur Polym J 45: 1777–1784
34. Simon GP (1994) Dielectric relaxation spectroscopy of thermoplastic polymers and blends. Mater Forum 18:235–264
35. Debnath S, De PP, Khastgir D (1988) Ambient electrical properties of mica-styrene-butadiene rubber composites. Rubber Chem Technol 61:555–567